Research Square

Preprints are preliminary reports that have not undergone peer review.
They should not be considered conclusive, used to inform clinical practice,
or referenced by the media as validated information.

KIF18A inhibition enhances glioma response to radiotherapy through activation of cGAS–STING signaling

Luohuan Dai
Xiangya Hospital Central South University
Wei Zhang
Xiangya Hospital Central South University
Hongwei Liu
Xiangya Hospital Central South University
Jia Gu
Xiangya Hospital Central South University
Yongwei Zhu
Xiangya Hospital Central South University
Abraham Ayodeji Adegboro
Xiangya Hospital Central South University
Hongyi Liu
Xiangya Hospital Central South University
Jiaqi Hao
Xiangya Hospital Central South University
Shunjun Xia
Xiangya Hospital Central South University
Deborah Oluwatosin Fasoranti
Xiangya Hospital Central South University
Nian Jiang
Xiangya Hospital Central South University
Kang Peng
Xiangya Hospital Central South University
Kexuan Zhong
Xiangya Hospital Central South University
Chubei Teng
Xiangya Hospital Central South University
Xuejun Li
lxjneuro@csu.edu.cn

Xiangya Hospital Central South University

Research Article

Keywords: Glioma, Radiotherapy, KIF18A, Radiosensitization, STING

Posted Date: October 5th, 2026

DOI: https://doi.org/10.21203/rs.3.rs-10935673/v1

License: This work is licensed under a Creative Commons Attribution 4.0 International License.
Read Full License

Additional Declarations: No competing interests reported.

Abstract

Background

Radioresistance remains a major cause of glioma recurrence, highlighting the need for therapeutically actionable radiosensitizing targets. Kinesin family member 18A (KIF18A), a mitotic motor protein essential for the survival of chromosomally unstable tumor cells, has emerged as a promising therapeutic target. However, its role and underlying mechanisms in regulating glioma radiosensitivity remain poorly understood. This study aims to evaluate the therapeutic potential and mechanisms of KIF18A inhibition combined with radiotherapy in glioma.

Methods

Integrated analyses of the Chinese Glioma Genome Atlas, The Cancer Genome Atlas and two public CRISPR/Cas9 screening platforms were performed to identify regulators of glioma radiosensitivity. KIF18A was genetically depleted using shRNA and pharmacologically inhibited with sovilnesib, a selective KIF18A inhibitor. Radiosensitizing effects were evaluated in glioma cell lines, patient-derived glioma stem cells, glioma organoids, and intracranial U251 and U87 xenograft models. To investigate the mechanism, Bulk RNA sequencing, STING inhibition with H151, and STING1 silencing were employed. An immunocompetent GL261 syngeneic glioma model was used to assess antitumor immune responses.

Results

KIF18A was identified as a novel regulator of glioma radiosensitivity, with elevated expression associated with poor survival among patients receiving radiotherapy. KIF18A knockdown enhanced radiosensitivity in U251, U87, and GL261 cells. Consistently, KIF18A knockdown combined with radiotherapy prolonged survival in U251 and U87 xenograft models. Moreover, the KIF18A inhibitor sovilnesib combined with irradiation suppressed proliferation of glioma cell lines and patient-derived primary and recurrent glioma cell lines. In patient-derived glioma organoids, combination treatment increased γH2AX-positive cells and decreased Ki-67-positive cells. It also significantly prolonged survival in U251 orthotopic models. Mechanistically, KIF18A inhibition increased radiation-induced micronuclei formation, leading to cytosolic double-stranded DNA accumulation and subsequent cGAS–STING pathway activation. This activation was accompanied by elevated cleaved caspase-3 levels and increased secretion of inflammatory mediators (TNF, CXCL3, and CXCL8). STING inhibition with H-151 or STING1 silencing attenuated the radiosensitizing effects. Notably, in immunocompetent GL261 models, combination treatment increased $CD8^+$ T-cell infiltration and promoted M1-like macrophage polarization.

Conclusion

KIF18A inhibition enhances glioma radiosensitivity by increasing DNA damage and activating cGAS–STING signaling. These findings highlight sovilnesib as a promising radiosensitizer for glioma.

Introduction

Glioma is the most lethal primary intracranial tumor, with a 5-year survival rate below 6%. Radiotherapy (50–60 Gy) combined with temozolomide following surgical resection constitutes the current standard of care[1, 2]. Despite intensive treatment, recurrence driven by radio-resistant tumor clones remains almost unavoidable[3, 4]. Radio-resistance arises from multiple factors, including genetic heterogeneity, altered genome stability, an immunosuppressive microenvironment, and the persistence of cancer stem cells[5].

Kinesin family member 18A (KIF18A), a kinesin-8 motor protein, plays a crucial role in mitotic chromosome dynamics[6]. Localized on spindle microtubules, KIF18A uses ATP hydrolysis in its motor domain to move toward microtubule (MT) plus ends, facilitating chromosome alignment at the metaphase plate and ensuring accurate sister-chromatid separation[7–9]. Increasing evidence shows that overexpression of KIF18A has been reported in multiple malignancies-including hepatocellular carcinoma[10], prostate cancer[11], breast cancer[12], lung adenocarcinoma[13] and glioma[14, 15], as tumor cells harboring high levels of chromosomal instability (CIN) strongly depend on KIF18A for faithful mitotic progression[16–19]. Given that radiotherapy is a major inducer of CIN[20, 21], KIF18A may play an important role in regulating tumor responses to irradiation. However, whether and how KIF18A regulates radiosensitivity in glioma remains unknown.

Reflecting the essential function of KIF18A, several small-molecule KIF18A inhibitors have been developed, and three inhibitors—Sovilnesib (NCT04293094), VLS-1488 (NCT05902988), and GH2616 (NCT06329206)—have entered phase Ib clinical testing[15, 22]. Pharmacological or genetic inhibition of KIF18A disrupts mitotic fidelity and promotes micronucleus (MN) formation in CIN tumor cells. Rupture of MN results in cytosolic dsDNA accumulation, thereby activating the cyclic GMP-AMP synthase-stimulator of interferon genes (cGAS-STING) pathway[23]. Therefore, considering that radiation itself is a potent inducer of CIN[21], we hypothesized that KIF18A inhibition synergizes with radiotherapy to augment the cGAS–STING activation.

In this study, we integrated data from TCGA, CGGA and two public CRISPR/Cas9 screening databases to investigate the association between KIF18A expression and glioma radio-resistance. Using patient-derived organoids and intracranial xenograft and allograft models, we further confirmed that suppressing KIF18A enhances the therapeutic response to radiotherapy.

Methods

Patient samples and cell culture

A cohort consisting of seven GBM samples with matched adjacent tissues and nineteen recurrent GBMs with paired primary tumors was collected from Xiangya Hospital, Central South University. All patients provided informed consent, and sample collection was approved by the Medical Ethics Committee of Central South University. Patient-derived GBM cell lines (GBM001, GBM005, GBM014, GBM017, GBM017R, GBM018, GBM040, GBM044) were established at Xiangya Hospital. Standard glioblastoma cell lines (U251, U87, U118, A172, LN229, GL261) and HEK293T cells were obtained from the Cancer Research Institute of Central South University. Patient-derived GBM cells were maintained in Neurocult NS-A basal medium (Stemcell Technologies, #05750) supplemented with 2 mM L-glutamine (Wisent, #609-065-EL), 75 μg/ml BSA (Life Technologies, #15260-037), B27 supplement without vitamin A (Gibco, #12587010), N2 supplement (Gibco, #17502048), 10 ng/ml rhEGF (Sigma-Aldrich, #E9644), 10 ng/ml bFGF (PeproTech, #100-18B), and 2 μg/ml heparin (Sigma-Aldrich, #H3149) [24]. Standard GBM cell lines and HEK293T cells were cultured in DMEM (Bio-Channel, #BC-M-005) containing 10% FBS (Pricella, #164210-50).

Generation of glioblastoma organoids (GBO)

GBOs were generated following previously described protocols[25, 26]. Six patient samples were processed in total. Under a stereomicroscope, tissues were cut into 0.2–0.5 mm fragments using microsurgical scissors (Anikas, Taobao). The fragments were transferred to ultra–low attachment six-well plates (Biofil, #TCP030006) containing 4 ml GBO medium composed of 50% Neurobasal medium (Thermo, #21103049) and 50% DMEM/F12 (Gibco, #C11330500BT), supplemented with MEM-NEAAs (Thermo, #11140050), GlutaMAX (Thermo, #35050061), N2, B27, human insulin (MCE, #HY-P0035), 2-mercaptoethanol (Thermo, #21985023), and 1% Pen-Strep (Thermo, #15070063). Cultures were maintained on an orbital shaker at 120 rpm. After 1–2 weeks, spherical and healthy GBOs were selected and randomly assigned to three groups: DMSO, DMSO_IR, and sovilnesib_IR. Organoids were treated with 5 μM sovilnesib for 3 days, followed by 2 Gy irradiation, and were harvested 24 hours after treatment.

Immunofluorescence staining

Cells grown on coverslips were fixed by precooled 4% PFA for 15 min. GBOs were harvested, fixed in precooled 4%PFA, and then dehydrated in 30% sucrose solution for 24 hours. They were later embedded in OCT and cut into 5-μm cryo-sections. Sections were then permeabilized by 0.1% Triton-X 100 in DPBS for 20 min, and blocked by 5% BSA for 1 hour. The cells were incubated with primary antibody overnight at 4 ℃, secondary antibody at dark RT for 1 hour, and DAPI for 5 min. Each step was followed by three washes in DPBS (3 min each). All antibodies were diluted by 1% BSA and 0.1% Triton-X 100 in DPBS. Images were observed by ZEISS LSM 900 confocal microscope. The antibodies used were: rabbit anti-KIF18A (Bethyl #A301-080A, 1:200), rabbit anti-γH2AX (Cell signaling technology #9718S, 1:500), mouse anti-Ki67 (Cell signaling technology #9449S, 1:1,000), mouse anti-Lamin A/C (Cell signaling technology #4777S, 1:200), mouse anti-dsDNA (Santa #HYB331-01, 1:100), rabbit anti-STING (Proteintech #19851-1-AP, 1:100), rabbit anti-cGAS (CST #79978, 1:200), rabbit anti-Tom20 (CST #79978, 1:200), rabbit anti-

γH2AX (1:500), mouse anti-Ki67 (1:500), conjugated to Alexa Fluor 488 and 555 (Invitrogen #A32766; #A32794, 1:1,000).

Immunohistochemistry

Patient and animal samples were fixed in 4% PFA for 24 hours, paraffin embedded and cut into 5 μm sections. After heating, deparaffinization, and hydration, the antigen was repaired using 10 nM citrate buffer at 95 ℃ for 15 min. 10% donkey serum was blocked for 30 min. The rabbit anti-KIF18A primary antibody (1:200), CD3 (ab237721, 1:1000) and CD8 (ab209775, 1:1000) were incubated at 4 ℃ for 12 hours, secondary antibody was incubated at room temperature (RT) for 20 min, and DAB was used for 5 min. All histological and immunohistochemical sections were reviewed by a pathologist to assess tissue morphology and potential treatment-associated toxicological changes.

Western Blotting

Western Blotting
Total protein was extracted with RIPA lysis solution (Beyotime) and 1% DMSF (Beyotime). Lysates were placed on ice for 30 min, sonicated, and then centrifuged at 13,300 rpm for 15 min at 4 ℃. 15μg-30μg protein samples per well were separated by 10%-12% SDS-polyacrylamide gel electrophoresis (SDS-PAGE) at 120V for 90min, then transferred to 0.22 μm PVDF membranes at 300 V for 50 min and blocked with 5% BSA and 0.1% Tween-20 in PBS. Finally, the membranes were incubated with primary antibody, secondary antibody and ECL buffer. The images were observed by Bio-Rad Chemidoc imaging system. Three biological replicates were performed for each quantitative data. The antibodies used were: rabbit anti-KIF18A (1:5,000), rabbit anti-γH2AX (1:1,000), Mouse anti-GAPDH (ABclonal #AC033, 1:10,000), rabbit anti-Rad51 (CST #8875S, 1:200), HRP-conjugated goat anti-rabbit (servicebio # gb23303, 1:5,000), and HRP-conjugated goat anti-mouse (servicebio # gb23301, 1:10,000).

Multiplex immunohistochemistry

Paraffin-embedded tissue sections were deparaffinized and rehydrated. Then heat-induced epitope retrieval was performed, followed by blocking with 3% hydrogen peroxide solution for 25 min and 10% rabbit serum or 3% BSA for 30 min. Finally, we used a multiplex immunohistochemistry (mIHC) kit (TSA kit AAT bio) to stain Iba1 (abcam, #ab178846, 1:8000), iNOS (boster, #BA0362, 1:200), and Cd206 (CST, #24595, 1:2000) in tissue sections. Briefly, after incubating the first primary antibody at 4°C overnight, the slide was incubated with the corresponding HRP labeled secondary antibody at room temperature for 50 min, and then incubated with the corresponding type of TSA working solution at room temperature for another 10 min. Subsequently, the sections were subjected to antigen retrieval again to prepare the next round of staining. Lastly, DAPI was used to mark the nucleus, and we used an OLYMPUS microscope for multispectral slice analysis under the appropriate fluorescent filters.

Real-time quantitative PCR

Total RNA was extracted using FlashPure Total RNA Mini Kit (GeneBetter), and then reversed transcribed into cDNA using the cDNA Synthesis Kit (Trans-Gen). Real-time quantitative PCR was performed using BRYT Green qPCR master Mix (Promega). Specific primers were: *KIF18A* (forward: CAAACTGCCGAACAACCAAAGC, reverse: TTCCACCTGAAGATGAGCAACAAG); *GAPDH* (forward: CTCCTGCACCACCAACTGCT, reverse: GGGCCATCCACAGTCTTCTG); *Kif18a* (forward: CGAGAAGGAATCAGGCAAGAGTATC, reverse: ATCTCTATCTGTTTATGGCACTGTTGG); *Gapdh* (forward: CATGGCCTTCCGTGTTCCTA, reverse: CCTGCTTCACCACCTTCTTGAT). RNA abundance was calculated using the 2-ΔΔCT method.

Lentivirus shRNA transfection and siRNA transfection

KIF18A knockdown was achieved using pLKO.1-based shRNA lentiviral vectors. HEK293T cells were co-transfected with the shRNA plasmid, PAX2, and PDM2.G packaging plasmids at a ratio of 4:3:1 using standard transfection procedures. The supernatant was harvested for 72 hours and centrifuged to obtain Lentiviruses. KIF18A overexpressing Lentiviruses were bought from Shanghai Genechem (#GV492). Lentiviruses were transfected into cells in antibiotic-free medium for 72 hours and Puromycin selection followed for 3 days. STING1 siRNA was transfected into cells using Lipofectamine 3000 for 8 h, followed by replacement with fresh complete culture medium. Human *KIF18A* shRNA antisense sequences are: #1: AAGAGAATCCTTTAACAAGCG, #2: TTGTGCCTTCTACAAATCGGG, scramble shRNA antisense is ACGCGTGCATACCTGCGG. Mouse *Kif18a* shRNA antisense sequence is: #2: GATGCTGTCTTTGATGAAACT, scramble shRNA antisense is TTCTCCGAACGTGTCACGT. STING1 siRNA antisense sequence is: CAUAGAUGCUGUUGCUGUAAACCCG, Negative control antisense sequence is: ACGUGACACGUUCGGAGAA.

Cell counting kit-8 (CCK8) for radiation survival fraction

500 cells per well were seeded. On day 2, inhibitor sovilnesib with IC_{50} concentration was added, and on the 3rd day, 6 Gy radiation was performed. Subsequently, the absorbance (OD value) at 450 nm was measured using Molecular Devices SpectraMax ABS Plus on days 0, 1, 2, 3, 4 after radiotherapy. 10 μL of CCK-8 reagent (MeilunBio, #MA0218) was added to each well and placed in the incubator for 2 hours. The cell surviving fraction was determined by normalizing the OD value of the radiotherapy group to day 0 and comparing it to the non-radiotherapy group.

Clone for radiation survival fraction

1000 cells/well were seeded in 6-well plates for 24 hours after treating with 0, 3, 6, 9 Gy radiation. After culturing for 14 days, cells were fixed with 4% PFA for 30 min, stained with 0.1% crystal violet for 30 min, and washed with running water. The survival fraction was determined by normalizing the colony

formation of irradiated cells to the number of seeded cells and comparing it to the non-irradiated group. The dose enhancement rations (DERs) was calculated at the survival fraction of 50%.

Xenograft, radiation therapy and sovilnesib administration

Glioma Cells with luciferase were transfected with the sh-lentivirus and selected by puromycin for 3 days. 250,000 U251 or U87 cells in 5 μL were orthotopically injected into 6-week-old female BALB/c-Nude mice from GemPharmatech. 10,000 GL261 cells were orthotopically injected into 6-week-old female C57BL/6J mice. The injection location was 2 mm behind the bregma, 1 mm at right lateral side and 2.5 mm depth. After alcohol iodine disinfection, the skin was bonded with tissue glue. When the tumor volume was detected to be appropriate by bioluminescence, the mice were randomly divided into control, control_radiation, shKIF18A and shKIF18A_radiation groups. Mice in the radiation group were treated with 3 Gy irradiation for 3 days. Sovilnesib was dissolved in a vehicle consisting of 5% DMSO, 40% PFG300, 5% Tween-80, and 50% PBS, and administered intraperitoneally at 30 mg/kg.

Bioinformatics

Datasets and data processing

The glioma RNA-seq date and clinical information were downloaded from the Chinese Glioma Genomic Atlas (CGGA, http://www.cgga.org.cn/), the Clinical Proteomic Tumor Analysis Consortium (CPTAC, https://proteomics.cancer.gov/programs/cptac), the Cancer Genome Atlas (TCGA, https://tcga-data.nci.nih.gov/) and the Gene Expression Omnibus databases (GEO, https://www.ncbi.nlm.nih.gov/gds/). The genome-wide CRISPR-Cas9 screening data of glioma was acquired from the Depmap (https://depmap.org/portal/download/)[27] and the work of Zhu. et al.[28]. In addition, a single cell RNA-seq dataset (EGAS00001005300) [29] and other glioma cohorts' transcript dataset (GSE4290, GSE16011, GSE35493, GSE43378) were collected. The parameters in the single-cell analysis were consistent with those published in the references[29]. For the GEO microarray datasets, data preprocessing was carried out with R package affy (version 1.72.0).

Investigating the association between KIF18A and radiosensitivity in Gliomas

We initially compiled a comprehensive list of 16565 protein-coding genes. Subsequently, we utilized the RNA-seq data from the Chinese Glioma Genome Atlas (CGGA) to enroll primary gliomas that had undergone radiotherapy alone, in order to identify potential factors associated with radiosensitivity. We stratified the cohort into radiotherapy-resistant gliomas and radiotherapy-sensitive gliomas based on the median time of overall survival. We defined patients with survival longer than the median survival as the sensitive group. We utilized the R package limma (version 3.48.0) to identify differentially expressed genes between the two groups, with a significance threshold of adjusted $P < 0.05$ and logFC > 0. Subsequently, univariate Cox regression analysis was conducted to determine the targets that were negatively correlated with survival outcomes, using criteria of adjusted $P < 0.05$ and HR > 1. A comprehensive whole-genome CRISPR screening approach was employed to identify the mediators

conferring irradiation resistance in glioma, specifically utilizing the U251 cell line. Subsequently, we generated a panel of irradiation resistance mediators by intersecting the genes exhibiting the top 10% sgRNA abundance with those genes demonstrating sgRNA diversity greater than 3 within U251 cells. We calculated the CERES scores of approximately 17,000 genes in DepMap datasets to investigate gene dependency. Candidate genes were defined as essential genes with a CERES score less than − 1 across 75% of glioma or glioblastoma cell lines. Through these methods, we ultimately determined that *KIF18A* is a key factor that can worsen the prognosis of glioma patients and facilitates radiotherapy resistance.

Bulk RNA sequencing analysis

Raw sequencing data derived from U251 cell line were mapped to hg38 reference genomes respectively by using HISAT2 toolkit (version 2.2.1). We used R package DESeq2 (version 1.32.0) to detect differentially expressed genes between control and treated U251. Differentially expressed genes with adjusted *P*-value < 0.05 and |log2(fold change) | > 0.5 were accepted as significant. And these genes were sorted by log2(fold change) as input to the GSEA algorithm in R package clusterProfiler (version 4.7.1) for GO and KEGG enrichment analysis. NES > 0 means up-regulated biological processes in treated U251, while NES < 0 means down-regulated biological processes in treated U251.

Data statistics analysis

All experiments were performed with at least three independent biological replicates. Two-groups samples were compared using the two-tailed student's t test. Multi-group samples were analyzed using One-Way ANOVA analyses. Survival differences were assessed by applying the Log-rank test. *P*-values less than 0.05 were considered statistically significant. All Statistical analyses and graphs were generated with GraphPad Prism (version 10.0) and R software (version 4.1.3).

Results

Overexpression of KIF18A in glioma predicts poor radiotherapy prognosis

To identify genes associated with poor prognosis in glioma patients who received radiotherapy, we analyzed transcriptomic and clinical data from the CGGA.326 and CGGA.693 cohorts. A total of 5802 differentially expressed genes were identified between radio-sensitive and radio-resistant patients, among which 683 genes showed a negative association with survival. These candidates were subsequently filtered by Genome-scale CRISPR/Cas9 gain-of-function screening for radiation resistance, followed by validation through loss-of-function screening. As a result, *KIF18A* emerged as a key gene required for glioma cell survival under radiotherapeutic stress (Fig. 1A, Supplementary Table 1).

Consistent findings across multiple large cohorts showed that *KIF18A* expression was elevated in glioma compared with normal brain tissue, and increased progressively with WHO tumor grade (Fig. 1B, C, Supplementary Fig. 1A, B). Both mRNA and protein levels of KIF18A were markedly higher in glioma tissues relative to adjacent non-tumor brain from the same patients (Fig. 1C-E). In addition, single-cell transcriptomic profiling revealed that proliferating stem-cell-like populations and G2/M-phase tumor

cells express high levels of *KIF18A* (Fig. 1F, supplementary Fig. 1C), supporting its association with malignant progression.

Through analyzing the CGGA and TCGA databases, we found that recurrent and secondary gliomas previously treated with radiotherapy displayed higher *KIF18A* expression than primary gliomas (Fig. 1G). This trend was validated at the protein level using matched samples, where recurrent gliomas (n = 19) exhibited an increase in KIF18A expression compared with primary gliomas ($p < 0.05$) (Fig. 1H). Furthermore, Kaplan-Meier analysis across multiple cohorts showed that high *KIF18A* expression was associated with significantly shorter overall survival in radiotherapy-treated patients ($p < 0.01$) (Fig. 1I). In contrast, no significant survival difference was observed in patients treated with temozolomide alone (Supplementary Fig. 1D), highlighting potential role of KIF18A in radioresistance. Because glioma prognosis is strongly influenced by histopathological subtype and tumor grade, we further stratified the patient cohorts according to pathological classification. High KIF18A expression was associated with poor treatment outcomes in astrocytoma, whereas its prognostic significance was less evident in glioblastoma, possibly due to the limited sample size. Nevertheless, in glioblastoma patients receiving combined radiotherapy and chemotherapy, high KIF18A expression showed a trend toward poorer prognosis (Supplementary Fig. 2A, B). Further multivariate Cox regression analysis indicated that KIF18A may serve as a potential risk factor, although the association did not reach statistical significance ($p > 0.05$) (Supplementary Fig. 1E). Taken together, our findings indicate that upregulation of *KIF18A* is associated with higher pathological grade and predicts poor prognosis in glioma patients following radiotherapy.

Knockdown of KIF18A increases the radiation sensitivity of glioma cells in vitro

To study the role of KIF18A in glioma radiotherapy, glioma cell lines U251, U87 and GL261 were exposed to ionizing radiation. KIF18A expression increased at 12 and 24 hours post-irradiation (Fig. 2A-B). We then generated *KIF18A*-knockdown cells (Fig. 2C, Supplementary Fig. 3A). CCK-8 assays showed that loss of *KIF18A* significantly enhanced the time-course radiation sensitivity ($p < 0.0001$) (Fig. 2D). Similarly, clone formation assays showed a marked increase in dose-dependent radiosensitivity ($p < 0.01$) following KIF18A depletion (Fig. 2E, F). Conversely, overexpression of KIF18A significantly increased the radioresistance in U251 and U87 cells (Supplementary Fig. 3B-D).

Knockdown of KIF18A improves the therapeutic response to radiotherapy in glioma xenograft models

To determine whether *KIF18A* knockdown improves radiotherapy efficacy *in vivo*, we established intracranial glioma models. Detailed radiotherapy and bioluminescence steps are shown in Fig. 3A. The shKIF18A_IR group displayed the lowest fluorescence volume, showing a rapid decline following irradiation (Fig. 3B-E). Notably, the combination of shKIF18A and radiotherapy contributed to the greatest survival benefit. In U87 tumor-bearing mice, the median survival of the shKIF18A_IR group was extended by 10.4% compared with the radiotherapy-alone group ($p < 0.05$) (Fig. 3F). In U251 tumor-bearing mice, KIF18A knockdown yielded an even greater improvement, prolonging median survival by 23.8% relative to the radiotherapy-alone group ($p < 0.05$) (Fig. 3G). Consistently, H&E staining showed that mice

receiving the combination treatment developed the smallest tumor burden (Fig. 3H-I). Collectively, these results revealed *KIF18A* knockdown significantly sensitizes glioma cells to radiotherapy both *in vitro* and *in vivo*.

The KIF18A inhibitor sovilnesib sensitizes glioma cells and patient-derived organoids to radiotherapy

Sovilnesib (AMG650) is a KIF18A-targeting inhibitor that binds the motor α4 and α6 helices within the kinesin motor domain of KIF18A and is currently in Phase clinical trials for ovarian and breast cancer (NCT04293094)[30]. However, its therapeutic potential in glioma has not been previously examined. To assess it efficacy, we first evaluated the drug response of six standard glioma cell lines and eight patient-derived glioma stem cell lines. Under 2 Gy irradiation, sovilnesib exhibited a concentration-dependent growth inhibition across all tested cell lines, with most IC_{50} values falling below 5 μM. U251, GBM001, GBM017R, and GBM018 cells exhibited the highest sensitivity, with IC_{50} values of approximately 1 μM (Fig. 4A, Supplementary Table 3). CCK-8 and clone formation assays showed that sovilnesib suppressed cell proliferation and significantly increased radiosensitivity ($p < 0.05$) (Fig. 4B, C). The dose enhancement rations (DERs) of U251, U87, and GL261 cells were 2.34, 2.67 and 1.12, respectively (Fig. 4C).

Glioblastoma (GBM) organoids, which recapitulate key structural and microenvironmental properties of tumors, provide a valuable platform for drug evaluation[31, 32]. To investigate whether sovilnesib exerts similar radiosensitizing effect in patient's tumor, we generated 6 GBM organoids (characterization shown in Supplementary Fig. 4). Organoids were treated for three days with radiation alone or sovilnesib plus radiation (Fig. 4D). Immunofluorescence staining revealed a progressive reduction in Ki-67 levels from untreated to combination-treated group, whereas γH2AX levels increased accordingly, indicating enhanced DNA damage in the presence of sovilnesib (Fig. 4E).

Sovilnesib prolongs the median survival of glioma xenograft models

To further evaluate the therapeutic efficacy of sovilnesib *in vivo*, we administered sovilnesib in intracranial glioma xenograft models (Fig. 5A). Mice receiving the combination of sovilnesib and radiotherapy exhibited the lowest bioluminescence signal (Fig. 5B, C) and showed a significant survival benefit ($p < 0.05$) (Fig. 5D). Consistently, tumor burden in the combination group was the lowest (Fig. 5E). Importantly, H&E staining of major organs and cleaved caspase-3 immunohistochemistry of brain tissues showed no detectable toxicity associated with sovilnesib administration (Fig. 5F). Together, these findings demonstrate that pharmacological inhibition of KIF18A by sovilnesib robustly enhances the therapeutic response to radiotherapy.

KIF18A inhibition increases DNA damage and enhances activation of the cGAS-STING pathway

A key cytotoxic effect of radiotherapy is the induction of DNA double strand breaks (DSBs), which promote cell death [33, 34]. Silencing KIF18A markedly increased γH2AX foci 24 hours after irradiation ($p < 0.001$) (Fig. 6A–B), which was further supported by Western blotting showing increased γH2AX levels (Fig. 6C, Supplementary Fig. 5A). RAD51, a key mediator of homologous recombination repair of DNA double-strand breaks, was not significantly altered (Supplementary Fig. 5B). Based on this result, we performed Bulk RNA-sequencing 24 hours after irradiation (Fig. 6D). Principal component analysis (PCA) showed distinct transcriptional profiles (Fig. 6E). Comparative analysis using KEGG enrichment demonstrated significant upregulation of the cytosolic DNA-sensing pathway, including the cGAS–STING axis, in both shKIF18A versus scr.shRNA and shKIF18A_IR versus scr.shRNA_IR comparisons (Fig. 6F, Supplementary Table 2). Immune-related pathways were also enriched, including viral protein–cytokine interactions, TNF signaling, RIG-I–like receptor signaling, and chemokine signaling. Gene Ontology analysis similarly showed activation of innate immune responses, T-cell activation, and cell-killing processes (Fig. 6F). In the heatmap, we observed that the cGAS-STING pathway downstream genes, including *IKBKB* and *IRF*, and apoptosis genes, including *BAK1*, *CASP3* and *CASP9*, were upregulated. In contrast, the cGAS–STING inhibitor *ENPP1* and the anti-apoptotic gene *BCL2* were downregulated (Fig. 6G). RT-qPCR further confirmed increased expression of *IRF3* and multiple inflammatory cytokines, including *IFNB1*, *IL-6*, *TNF*, *CXCL3*, and *CXCL8* (Fig. 6H; Supplementary Fig. 5C).

KIF18A inhibition induces micronucleus formation to accelerate cGAS-STING pathway activation

To investigate the mechanism underlying the activation of the cGAS–STING pathway, we retrieved human KIF18A protein–protein interaction partners from the STRING database and performed functional enrichment analysis. Several interacting proteins, including CENPE, KIF11, KIF2C, CDC20, PLK1, AURKB, and TTK, were identified as spindle-associated motor proteins. Enrichment analysis further showed that these proteins were primarily associated with biological processes related to cell cycle regulation, spindle organization, and chromosome segregation (Supplementary Fig. 5D). Given that KIF18A deficiency disrupts chromosome segregation and that micronuclei are huge reservoirs of dsDNA capable of activating the cGAS-STING pathway[35–37], we next examined micronuclei formation by immunofluorescence. The combinational treatment produced more micronuclei than irradiation alone. We also observed lagging micronuclei between daughter nuclei in the combination group (Fig. 7A-B). Furthermore, combined treatment increased the number of cGAS foci, a hallmark of cGAS activation ($p < 0.05$), suggesting micronuclear rupture and exposure of dsDNA to the cytoplasm (Supplementary Fig. 6A). STING fluorescence intensity increased, and the number of cytosolic dsDNA foci rose significantly in the combination group ($p < 0.05$) (Fig. 7C–D). Notably, the dsDNA signal did not colocalize with the mitochondrial marker Tom20, suggesting that the cytosolic dsDNA was unlikely to be primarily derived from mitochondria (Supplementary Fig. 6C). In line with these findings, Western blotting further confirmed elevated phosphorylation of STING (Fig. 7E, F). Importantly, the STING inhibitor H151 and STING siRNA reversed the sensitizing effect of KIF18A inhibition on radiotherapy (Fig. 7G, H; supplementary 6D, E). These findings collectively demonstrate that KIF18A inhibition promotes

micronucleus formation and cGAS–STING pathway activation, thereby enhancing tumor-cell susceptibility to radiotherapy.

KIF18A inhibition enhances immune infiltration and macrophage M1 polarization

The cGAS–STING pathway is a key initiating signal for innate immune activation, and effective activation of this pathway can enhance antitumor immunity. Therefore, we leveraged a syngeneic GL261 glioma model to evaluate whether KIF18A inhibition could potentiate the immune effects of radiotherapy. Compared with radiotherapy alone, combined shKif18a and radiotherapy significantly prolonged the median survival ($p < 0.05$). Consistently, *in vivo* bioluminescence imaging showed comparable therapeutic responses (Fig. 8A–C). Immunohistochemical staining showed that combined treatment increased the infiltration of $CD8^+$ T cells ($p < 0.0001$), whereas T-cell infiltration was barely detectable in the control group (Fig. 8D). Given that myeloid cells constitute a major component of the glioma immune microenvironment, we further examined macrophage polarization. Combined treatment significantly increased the number of $IBA1^+$ $iNOS^+$ double-positive M1-like macrophages within the tumor ($p < 0.001$), whereas the number of $IBA1^+$ $CD206^+$ double-positive M2-like macrophages showed a consistent change (Fig. 8E). Taken together, these results suggest that KIF18A inhibition enhances radiotherapy-induced antitumor immunity in glioma.

Discussion

In this study, we found that inhibition of KIF18A sensitizes glioma cells to radiotherapy by increasing DNA damage and amplifying cGAS-STING pathway. In immunocompetent mice, the combination treatment also enhanced $CD8^+$ T-cell infiltration. KIF18A is known to support the survival of CIN cancer cells[16, 17], and its overexpression has been reported in several malignancies, including breast, prostate, colorectal, hepatic, lung, and brain cancers[11, 13, 38–41]. Our previous work suggested that *KIF18A* may facilitate the transition from LGG to GBM[42]. In addition, Bingyan et al. reported that KIF18A is a marker of poor prognosis in glioma[43]. Consistent with this, Stangeland et al.[44] reported that KIF18A is enriched in GBM stem cells, and Mathur et al. [45] further showed that it participates in neurodevelopmental programs underlying GBM lineage origins. However, its association with glioma recurrence, and radiotherapy response had not been systematically evaluated. In this study, our integrative analysis revealed that KIF18A expression increases with WHO grade and is associated with poor survival following radiotherapy. Moreover, KIF18A was the only overlapping gene between CRISPR gain- and loss-of-function screens, underscoring its potential relevance in radioresistance. This interpretation is further supported by previous studies showing elevated KIF18A in radioresistant prostate cancer cells and enhanced radiosensitivity following KIF18A silencing in esophageal cancer cells further support this concept[46, 47]. Consistent with these observations, we found that radiation induces KIF18A expression and that KIF18A depletion improves radiotherapeutic efficacy *in vitro* and *in vivo*.

Pharmacological targeting of KIF18A has emerged as a promising strategy in CIN-high tumors, with several small-molecule inhibitors, including BTB-1, Sovilnesib, VLS-1488, ISM9682A, GH2616, AM-5308, AM-1882 and VLS-1272 currently under development[18, 22, 23, 48–51]. Sovilnesib and VLS-1488 are among the earliest KIF18A-targeting inhibitors to enter clinical trial. Notably, VLS-1488 demonstrated a favorable tolerability and preliminary antitumor activity, with no patients experiencing grade > 3 treatment-related adverse events, and tumor shrinkage observed in 7 of 17 patients with ovarian cancer[52]. In addition, a recent study reported that JAK1-deficient head and neck squamous cell carcinoma CAL27 cells acquire radioresistance by enhancing G2/M cell-cycle arrest. Notably, sovilnesib counteracted this cell-cycle arrest, increased DNA damage, and markedly improved tumor radiosensitivity *in vivo*[53]. In this study, we verified that sovilnesib acts as a radiosensitizer using glioma cell lines, patient-derived stem cells, organoids, and intracranial xenografts. Collectively, these studies suggest that KIF18A inhibition may have broad radiosensitizing potential across multiple tumor types.

Mechanistically, we observed that KIF18A inhibition increased micronuclei formation, cytosolic dsDNA accumulation, and cGAS–STING activation following irradiation. These events are known triggers of caspase-dependent cell death pathways[54, 55]. Radiation itself induces segregation errors and generates CIN-high cell populations[20, 21, 56], which may explain the enhanced vulnerability of irradiated cells to KIF18A loss [17]. Interestingly, KIF18A inhibition also enhanced radiotherapy-induced immune activation, as evidenced by increased $CD8^+$ T-cell infiltration and macrophage M1 polarization. This is consistent with previous studies showing that KIF18A inhibition stimulates type I interferon responses and activates cGAS–STING signaling, thereby promoting $CD8^+$ T-cell infiltration[57]. Taken together, the radiosensitizing effect of KIF18A inhibition is driven by activating the cGAS–STING pathway and its downstream signaling cascades, as increased chromosome segregation errors and DNA damage promote the accumulation of cytosolic DNA. (Fig. 9).

Several limitations should be acknowledged. First, while micronuclei formation was increased, we did not directly quantify mitotic errors or CIN severity; future studies incorporating live-cell imaging and karyotypic analyses are warranted. Second, our study showed that KIF18A inhibition was particularly pronounced in U251 cells, which is a *TP53*-mutant cell line[58]. Consistently, prior PRISM screening showed preferential inhibitor activity in TP53-mutant backgrounds[22]. p53 has been reported to limit the proliferation of nondiploid cells after chromosome missegregation; therefore, loss or mutation of TP53 may allow CIN cells to propagate and become more dependent on mitotic regulators, KIF18A[59]. Given that CIN-high tumor cells are more vulnerable to KIF18A inhibition, further evaluation of KIF18A inhibitors in patient-derived primary glioma cells with diverse genetic backgrounds will be important for identifying patients that benefit from this therapeutic strategy. Third, given the immune activation and therapeutic efficacy observed in the syngeneic model, the immune-regulatory mechanisms underlying KIF18A inhibition-mediated radiosensitization warrant further investigation using single-cell RNA sequencing and spatial transcriptomic approaches.

Conclusion

In summary, KIF18A is highly expressed in gliomas following radiotherapy and serves as a predictor of poor prognosis. Across multiple preclinical glioma models, inhibition of KIF18A synergistically enhances the therapeutic effects of radiotherapy by strengthened cGAS–STING signaling. These findings identify KIF18A as a promising therapeutic target and highlight sovilnesib as a potential radiosensitizer for glioma.

Abbreviations

GBM
Glioblastoma
cGAS-STING
The cyclic GMP-AMP synthase-stimulator of interferon genes pathway
CIN
chromosomal instability
WGD
whole-genome doubling
MN
micronuclei
GBO
glioblastoma organoid
CCK-8
Cell Counting Kit-8 analysis
DMSO
Dimethyl sulfoxide
CGGA
the Chinese Glioma Genomic Atlas
TCGA
the Cancer Genome Atlas

Declarations

Ethics approval

All patients provided informed consent, and the collection of human samples was approved by the Medical Ethics Committee of Central South University (Approval No. 2025091560). All procedures involving human participants were conducted in accordance with the Declaration of Helsinki. All animal experiments were approved by the Medical Ethics Committee of Central South University (Approval No. 2025030625) and conducted in accordance with the guidelines of the International Council for Laboratory Animal Science (ICLAS).

Consent for publication

All authors have read and approved the final version of the manuscript and agreed to its submission to Cellular & Molecular Biology Letters for publication.

Competing interests

The authors declare no competing interests and no commercial relationship with any organization that has influenced the results of the experiment.

Supplementary data

Supplementary data related to this article are available online.

Funding

This work is supported by the National Natural Science Foundation of China (Grant No. 82270825, No. 82403354 and No, 82401593), Postdoctoral Fellowship Program of CPSF (NO. GZC20233155) and Hunan Provincial Nature Science Foundation (No. 2025JJ90287).

Author Contribution

L.H.D., W.Z., and H.W.L. designed the project, performed experiments, analyzed the data and wrote the manuscript. X.J.L. and C.B.T. conceived and supervised the project, and revised the manuscript. J.G., H.Y.L., and Y.W.Z performed experiments and helped collect and visualize the data. A.A.A., D.O.F., and K.X.Z. made significant contributions to the linguistic refinement of this article. J.Q.H., and S.J.X. packaged the lentivirus and validated the data in the project. N.J., and K.P. provided funding and lots of valuable advice.

Acknowledgement

We sincerely thank the Public Platform for Advanced Medical Research Instruments of Central South University, the Preventive Medicine Experimental Center of Xiangya School of Public Health and the Key Laboratory of Hunan Province in Neurodegenerative Disorders in providing research equipment and technical support. We thank Dr. Zujian Xiong for his assistance in the preparation of this manuscript. The authors also thank the Department of Radiology of Xiangya Hospital for providing radiation therapy equipment, and Biorender.com for help in drawing the schematic. The authors would like to acknowledge the following datasets: TCGA, CGGA, GTEx, CPTAC, IVYGAP, GSE4290, etc.

Data Availability

RNA-seq of U251 cell line have been deposited in the National Genomics Data Center (NGDC, https://ngdc.cncb.ac.cn/) under the accession number PRJCA036800 and released upon publication.

References

1. Ostrom QT, Price M, Neff C, Cioffi G, Waite KA, Kruchko C, et al. CBTRUS Statistical Report: Primary Brain and Other Central Nervous System Tumors Diagnosed in the United States in 2015–2019. Neurooncology. 2022;24(Supplement5):v1–95.
2. Tan AC, Ashley DM, López GY, Malinzak M, Friedman HS, Khasraw M. Management of glioblastoma: State of the art and future directions. Cancer J Clin. 2020;70(4):299–312.
3. Rapp M, Baernreuther J, Turowski B, Steiger H-J, Sabel M, Kamp MA. Recurrence Pattern Analysis of Primary Glioblastoma. World Neurosurg. 2017;103:733–40.
4. van Linde ME, Brahm CG, de Witt Hamer PC, Reijneveld JC, Bruynzeel AME, Vandertop WP, et al. Treatment outcome of patients with recurrent glioblastoma multiforme: a retrospective multicenter analysis. J Neurooncol. 2017;135(1):183–92.
5. Wu Y, Song Y, Wang R, Wang T. Molecular mechanisms of tumor resistance to radiotherapy. Mol Cancer. 2023;22(1).
6. Chen Q, Le X, Li Q, Liu S, Chen Z. Exploration of inhibitors targeting KIF18A with ploidy-specific lethality. Drug Discovery Today. 2024;29(10).
7. Mayr MI, Hummer S, Bormann J, Gruner T, Adio S, Woehlke G, et al. The human kinesin Kif18A is a motile microtubule depolymerase essential for chromosome congression. Curr Biol. 2007;17(6):488–98.
8. Stumpff J, von Dassow G, Wagenbach M, Asbury C, Wordeman L. The kinesin-8 motor Kif18A suppresses kinetochore movements to control mitotic chromosome alignment. Dev Cell. 2008;14(2):252–62.
9. Janssen LME, Averink TV, Blomen VA, Brummelkamp TR, Medema RH, Raaijmakers JA. Loss of Kif18A Results in Spindle Assembly Checkpoint Activation at Microtubule-Attached Kinetochores. Curr Biol. 2018;28(17):2685–e964.
10. Luo W, Liao M, Liao Y, Chen X, Huang C, Fan J et al. The role of kinesin KIF18A in the invasion and metastasis of hepatocellular carcinoma. World J Surg Oncol. 2018;16(1).
11. Zhang H, Shen T, Zhang Z, Li Y, Pan Z. Expression of KIF18A Is Associated with Increased Tumor Stage and Cell Proliferation in Prostate Cancer. Med Sci Monit. 2019;25:6418–28.
12. Zhang C, Zhu C, Chen H, Li L, Guo L, Jiang W et al. Kif18A is involved in human breast carcinogenesis. Carcinogenesis. 2010;31.
13. Zhong Y, Jiang L, Lin H, Li X, Long X, Zhou Y, et al. Overexpression of KIF18A promotes cell proliferation, inhibits apoptosis, and independently predicts unfavorable prognosis in lung

adenocarcinoma. IUBMB Life. 2019;71(7):942–55.
14. Wang LB, Zhang XB, Liu J, Liu QJ. The Proliferation of Glioblastoma Is Contributed to Kinesin Family Member 18A and Medical Data Analysis of GBM. Front Genet. 2022;13:858882.
15. Mohd Amin AS, Eastwood S, Pilcher C, Truong JQ, Foitzik R, Boag J et al. KIF18A inhibition: the next big player in the search for cancer therapeutics. Cancer Metastasis Rev. 2024;44(1).
16. Bielski CM, Zehir A, Penson AV, Donoghue MTA, Chatila W, Armenia J, et al. Genome doubling shapes the evolution and prognosis of advanced cancers. Nat Genet. 2018;50(8):1189–95.
17. Quinton RJ, DiDomizio A, Vittoria MA, Kotynkova K, Ticas CJ, Patel S, et al. Whole-genome doubling confers unique genetic vulnerabilities on tumour cells. Nature. 2021;590(7846):492–7.
18. Marquis C, Fonseca CL, Queen KA, Wood L, Vandal SE, Malaby HLH, et al. Chromosomally unstable tumor cells specifically require KIF18A for proliferation. Nat Commun. 2021;12(1):1213.
19. Cohen-Sharir Y, McFarland JM, Abdusamad M, Marquis C, Bernhard SV, Kazachkova M, et al. Aneuploidy renders cancer cells vulnerable to mitotic checkpoint inhibition. Nature. 2021;590(7846):486–91.
20. Bakhoum SF, Kabeche L, Wood MD, Laucius CD, Qu D, Laughney AM, et al. Numerical chromosomal instability mediates susceptibility to radiation treatment. Nat Commun. 2015;6:5990.
21. Cosper PF, Copeland SE, Tucker JB, Weaver BA. Chromosome Missegregation as a Modulator of Radiation Sensitivity. Semin Radiat Oncol. 2022;32(1):54–63.
22. Payton M, Belmontes B, Hanestad K, Moriguchi J, Chen K, McCarter JD, et al. Small-molecule inhibition of kinesin KIF18A reveals a mitotic vulnerability enriched in chromosomally unstable cancers. Nat Cancer. 2024;5(1):66–84.
23. Phillips AF, Zhang R, Jaffe M, Schulz R, Carty MC, Verma A, et al. Targeting chromosomally unstable tumors with a selective KIF18A inhibitor. Nat Commun. 2025;16(1):307.
24. Dong W, Fekete A, Chen X, Liu H, Beilhartz GL, Chen X, et al. A designer peptide against the EAG2–Kvβ2 potassium channel targets the interaction of cancer cells and neurons to treat glioblastoma. Nat Cancer. 2023;4(10):1418–36.
25. Jacob F, Ming G-l, Song H. Generation and biobanking of patient-derived glioblastoma organoids and their application in CAR T cell testing. Nat Protoc. 2020;15(12):4000–33.
26. Li G, Wang D, Zhai Y, Pan C, Zhang J, Wang C, et al. Glycometabolic reprogramming-induced XRCC1 lactylation confers therapeutic resistance in ALDH1A3-overexpressing glioblastoma. Cell Metabol. 2024;36(8):1696–e71010.
27. Meyers RM, Bryan JG, McFarland JM, Weir BA, Sizemore AE, Xu H, et al. Computational correction of copy number effect improves specificity of CRISPR–Cas9 essentiality screens in cancer cells. Nat Genet. 2017;49(12):1779–84.
28. Zhu G-d, Yu J, Sun Z-y, Chen Y, Zheng H-m, Lin M-l et al. Genome-wide CRISPR/Cas9 screening identifies CARHSP1 responsible for radiation resistance in glioblastoma. Cell Death Dis. 2021;12(8).

29. Johnson KC, Anderson KJ, Courtois ET, Gujar AD, Barthel FP, Varn FS, et al. Single-cell multimodal glioma analyses identify epigenetic regulators of cellular plasticity and environmental stress response. Nat Genet. 2021;53(10):1456–68.
30. Belmontes B, Moriguchi J, Chung G, Sun J, Ninniri MSS, Hanestad K et al. Discovery and preclinical characterization of AMG 650, a first-in-class inhibitor of kinesin KIF18A motor protein with potent activity against chromosomally unstable cancers. Cancer Res. 2023;83.
31. Kim J, Koo B-K, Knoblich JA. Human organoids: model systems for human biology and medicine. Nat Rev Mol Cell Biol. 2020;21(10):571–84.
32. Li M, Izpisua Belmonte JC. Organoids — Preclinical Models of Human Disease. N Engl J Med. 2019;380(6):569–79.
33. Gulston M, Fulford J, Jenner T, Lara Cd, O'Neill P. Clustered DNA damage induced by gamma radiation in human fibroblasts (HF19), hamster (V79-4) cells and plasmid DNA is revealed as Fpg and Nth sensitive sites. Nucleic acids research. 2002;30(15).
34. Zhang Y, Wang Y, Zhou D, Wang K, Wang X, Wang X, et al. Radiation-induced YAP activation confers glioma radioresistance via promoting FGF2 transcription and DNA damage repair. Oncogene. 2021;40(27):4580–91.
35. Sepaniac LA, Martin W, Dionne LA, Stearns TM, Reinholdt LG, Stumpff J. Micronuclei in Kif18a mutant mice form stable micronuclear envelopes and do not promote tumorigenesis. J Cell Biol. 2021;220(11).
36. Kwon J, Bakhoum SF. The Cytosolic DNA-Sensing cGAS-STING Pathway in Cancer. Cancer Discov. 2020;10(1):26–39.
37. Mackenzie KJ, Carroll P, Martin CA, Murina O, Fluteau A, Simpson DJ, et al. cGAS surveillance of micronuclei links genome instability to innate immunity. Nature. 2017;548(7668):461–5.
38. Li TF, Zeng HJ, Shan Z, Ye RY, Cheang TY, Zhang YJ, et al. Overexpression of kinesin superfamily members as prognostic biomarkers of breast cancer. Cancer Cell Int. 2020;20:123.
39. Nagahara M, Nishida N, Iwatsuki M, Ishimaru S, Mimori K, Tanaka F, et al. Kinesin 18A expression: clinical relevance to colorectal cancer progression. Int J Cancer. 2011;129(11):2543–52.
40. Liao W, Huang G, Liao Y, Yang J, Chen Q, Xiao S et al. High KIF18A expression correlates with unfavorable prognosis in primary hepatocellular carcinoma. Oncotarget. 2014;4.
41. Liu T, Yang K, Chen J, Qi L, Zhou X, Wang P. Comprehensive Pan-Cancer Analysis of KIF18A as a Marker for Prognosis and Immunity. Biomolecules. 2023;13(2).
42. Teng C, Zhu Y, Li Y, Dai L, Pan Z, Wanggou S et al. Recurrence- and Malignant Progression-Associated Biomarkers in Low-Grade Gliomas and Their Roles in Immunotherapy. Front Immunol. 2022;13.
43. Tao BY, Liu YY, Liu HY, Zhang ZH, Guan YQ, Wang H, et al. Prognostic Biomarker KIF18A and Its Correlations With Immune Infiltrates and Mitosis in Glioma. Front Genet. 2022;13:852049.

44. Stangeland B, Mughal AA, Grieg Z, Sandberg CJ, Joel M, Nygård S et al. Combined expressional analysis, bioinformatics and targeted proteomics identify new potential therapeutic targets in glioblastoma stem cells. oncotarget. 2015;6(28).
45. Mathur R, Wang Q, Schupp PG, Nikolic A, Hilz S, Hong C, et al. Glioblastoma evolution and heterogeneity from a 3D whole-tumor perspective. Cell. 2024;187(2):446–63. e16.
46. Cai F, Li J, Zhang J, Huang S. Knockdown of Circ_CCNB2 Sensitizes Prostate Cancer to Radiation Through Repressing Autophagy by the miR-30b-5p/KIF18A Axis. Cancer Biother Radiopharm. 2022;37(6):480–93.
47. Qian L-X, Cao X, Du M-Y, Ma C-X, Zhu H-M, Peng Y, et al. KIF18A knockdown reduces proliferation, migration, invasion and enhances radiosensitivity of esophageal cancer. Biochem Biophys Res Commun. 2021;557:192–8.
48. Catarinella M, Grüner T, Strittmatter T, Marx A, Mayer TU. BTB-1: A Small Molecule Inhibitor of the Mitotic Motor Protein Kif18A. Angew Chem Int Ed. 2009;48(48):9072–6.
49. Tamayo NA, Bourbeau MP, Allen JR, Ashton KS, Chen JJ, Kaller MR, et al. Targeting the Mitotic Kinesin KIF18A in Chromosomally Unstable Cancers: Hit Optimization Toward an In Vivo Chemical Probe. J Med Chem. 2022;65(6):4972–90.
50. Zhang R, Cogan DA, Eng C, Phillips A, Carty MC, Feinberg T et al. Discovery of potent, orally active KIF18A inhibitors targeting CIN-high cancer cells. J Clin Oncol. 2022;40.
51. Zhang J, Gao F, Zhu W, Xu C, Ding X, Shang J et al. ISM9682A, a novel and potent KIF18A inhibitor, shows robust antitumor effects against chromosomally unstable cancers. Proceedings of the American Association for Cancer Research Annual Meeting. 2024;84.
52. Therapeutics V, editor. Preliminary Results from a First-in-Human, Phase I/II Study of VLS-1488, an Oral KIF18A Inhibitor, in Patients with Advanced Solid Tumors. American Society of Clinical Oncology (ASCO); 2025 2025.
53. Kelley VM, Baro M, Gasperi WE, Ader NR, Lea H, Lee H, et al. Loss of JAK1 Function Causes G2/M Cell Cycle Defects Vulnerable to KIF18A Inhibition. Cancer Res. 2026;86(8):2301–17.
54. Zierhut C, Villunger A. Mitotic lethality prevents inflammation. Nat Cell Biol. 2025;27(1):7–8.
55. Szmyd R, Casolin S, French L, Manjon AG, Walter M, Cavalli L, et al. Homologous recombination promotes non-immunogenic mitotic cell death upon DNA damage. Nat Cell Biol. 2025;27(1):59–72.
56. Storchova Z, Pellman D. From polyploidy to aneuploidy, genome instability and cancer. Nat Rev Mol Cell Biol. 2004;5(1):45–54.
57. Liu G, Zhang Y, Cao Z, Zhao Z. Targeting KIF18A triggers antitumor immunity and enhances efficiency of PD-1 blockade in colorectal cancer with chromosomal instability phenotype. Cell Death Discov. 2025;11(1):130.
58. Godoy PRDV, Mello SS, Magalhães DAR, Donaires FS, Nicolucci P, Donadi EA, et al. Ionizing radiation-induced gene expression changes in TP53 proficient and deficient glioblastoma cell lines. Mutat Research/Genetic Toxicol Environ Mutagen. 2013;756(1–2):46–55.

59. Thompson SL, Compton DA. Proliferation of aneuploid human cells is limited by a p53-dependent mechanism. J Cell Biol. 2010;188(3):369–81.

60. Bielski CM, Taylor BS. Homing in on genomic instability as a therapeutic target in cancer. Nat Commun. 2021;12(1):3663.

Figures

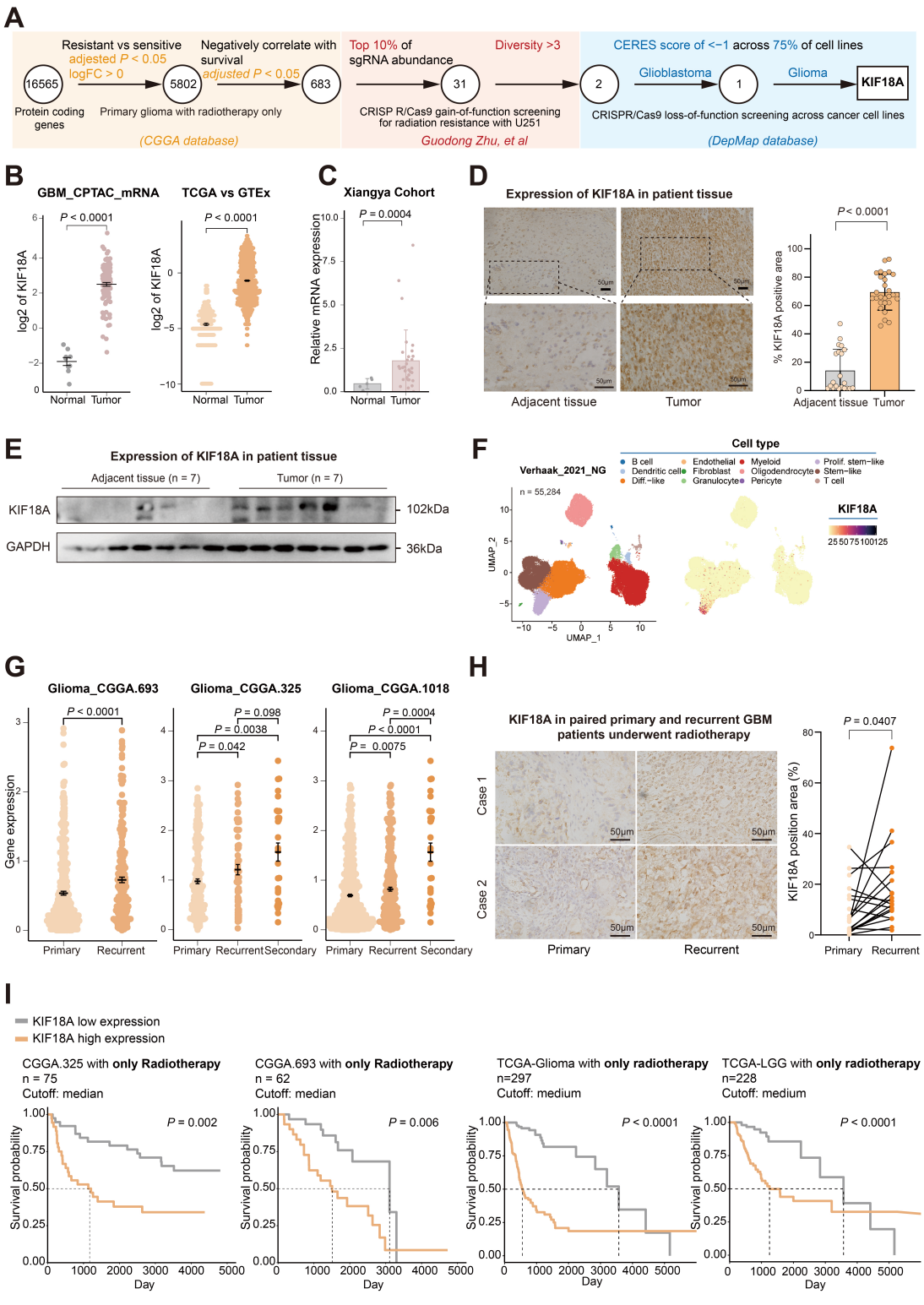


Figure 1

Overexpression of *KIF18A* in glioma predicts poor radiotherapy prognosis

A. Schematic workflow illustrating the screening strategy for identifying genes associated with glioma radioresistance using CGGA datasets and public CRISPR/Cas9 databases.

B. *KIF18A* mRNA expression in normal brain and glioma tissues across the CPTAC, TCGA, and GTEx datasets.

C. *KIF18A* mRNA expression in normal brain (n = 5) and glioma tissues (n = 30) from the Xiangya cohort.

D.Representative immunohistochemical images and quantification of KIF18A protein levels in adjacent non-tumor tissue versus tumor tissue. Each dot represents one field of view.

E.Western blotting analysis showing KIF18A protein levels in paired adjacent and tumor tissues (n = 7).

F.UMAP plots representing expression of *KIF18A*.

G. *KIF18A* mRNA expression in primary, recurrent, and secondary gliomas in the CGGA datasets.

H.Representative images and quantification of KIF18A protein levels in paired recurrent GBM samples (n = 19).

I.Kaplan–Meier survival curves of glioma patients receiving radiotherapy, stratified by high versus low KIF18A expression in the CGGA and TCGA datasets. Statistical analyses: Student’s t-test (C, D) and paired t-test (H). Data represent mean ± SD.

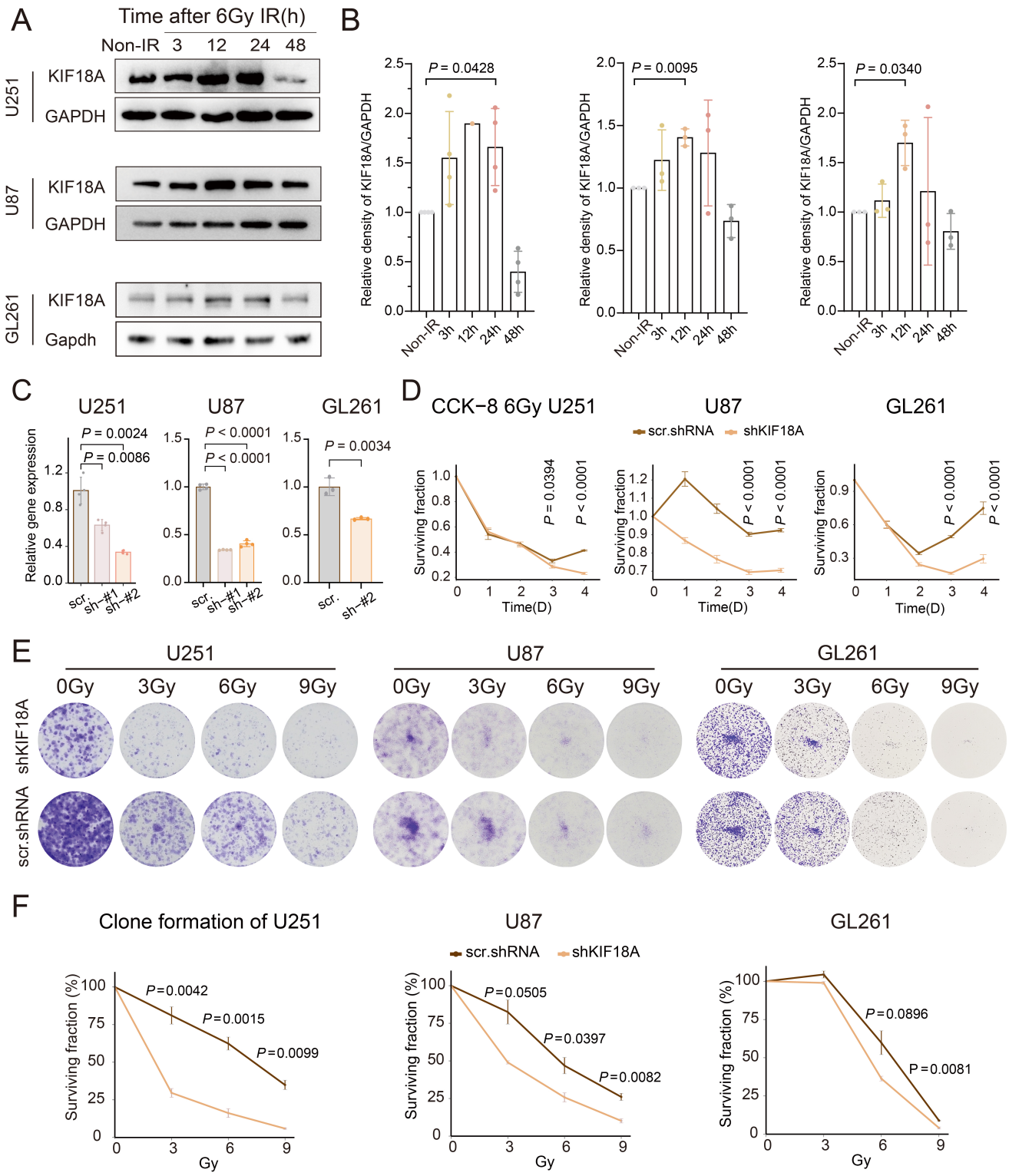


Figure 2

Knockdown of *KIF18A* increases the radiation sensitivity of glioma cells *in vitro*

A.Western blotting analysis of KIF18A expression in U251, U87, and GL261 cells following 6 Gy irradiation and collection within 48 hours.

B.Quantification of KIF18A protein levels after irradiation in U251, U87, and GL261 cells (n = 3–4).

C.RT–qPCR validation of KIF18A knockdown using shRNA lentiviral transduction.

D.Time-course survival curves of KIF18A-knockdown U251, U87, and GL261 cells following 6 Gy irradiation (n = 6).

E.Representative colony formation images of control and KIF18A-knockdown U251, U87 and GL261 cells after irradiation.

F. Quantification of colony numbers (n = 3). Statistical analyses: Student's t-test (B, C, D and F). Data represent mean ± SD.

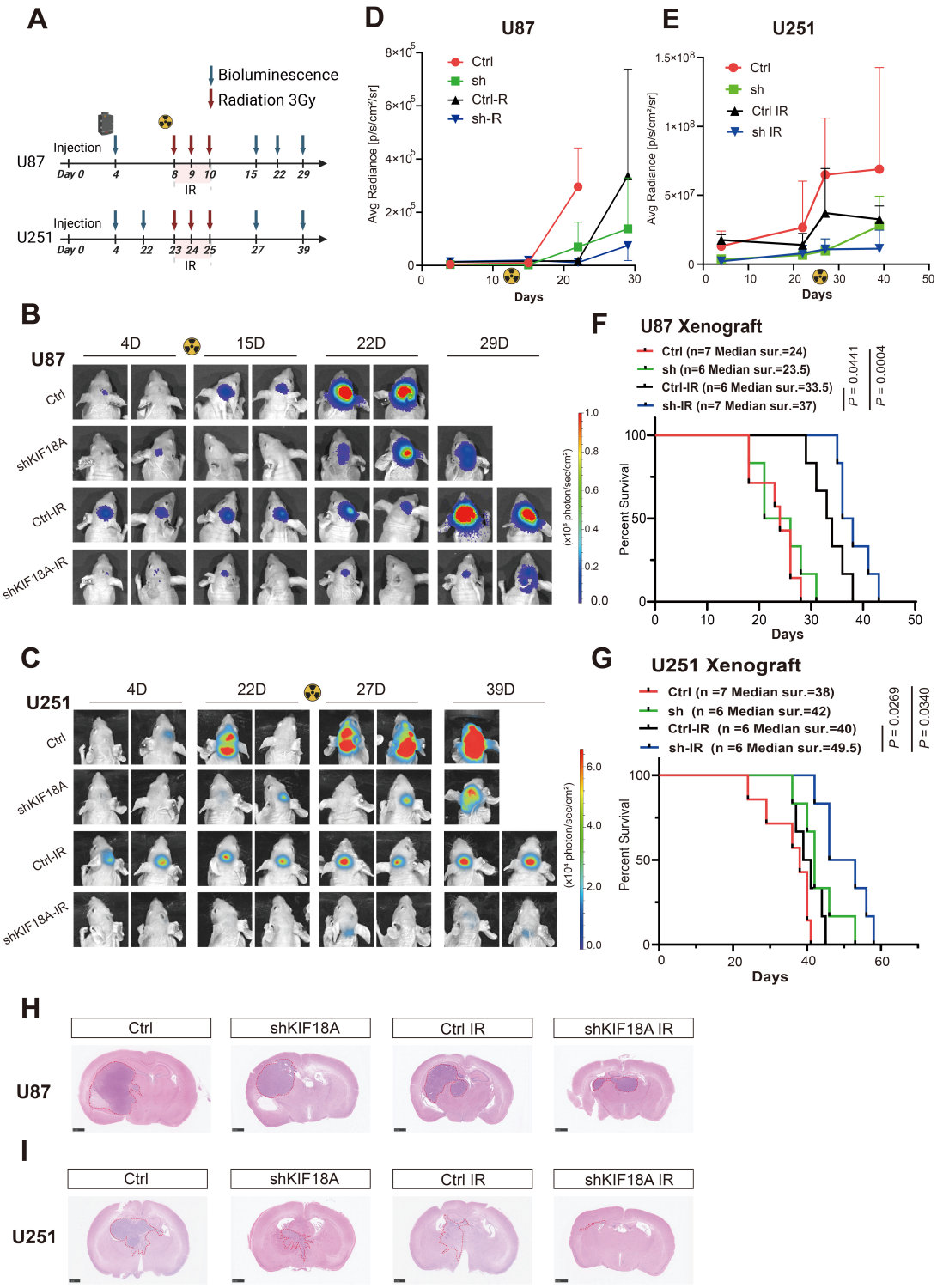


Figure 3

Knockdown of *KIF18A* improves the therapeutic response to radiotherapy in glioma xenograft models

A. Schematic illustration of treating the glioma xenograft models with radiotherapy.

B-C. Representative bioluminescence images of U87 (B) and U251 (C) intracranial xenografts.

D-E. Quantification of bioluminescent tumor signal in mice bearing U87 (D) and U251 (E) xenografts. Data represent mean ± SD.

F-G. Kaplan–Meier survival curves of mice bearing U87 (F) and U251 (G) xenografts (n = 6–7).

H-I. Representative H&E staining of U87 (H; day 25) and U251 (I; day 30) xenografts from control and KIF18A-knockdown groups.

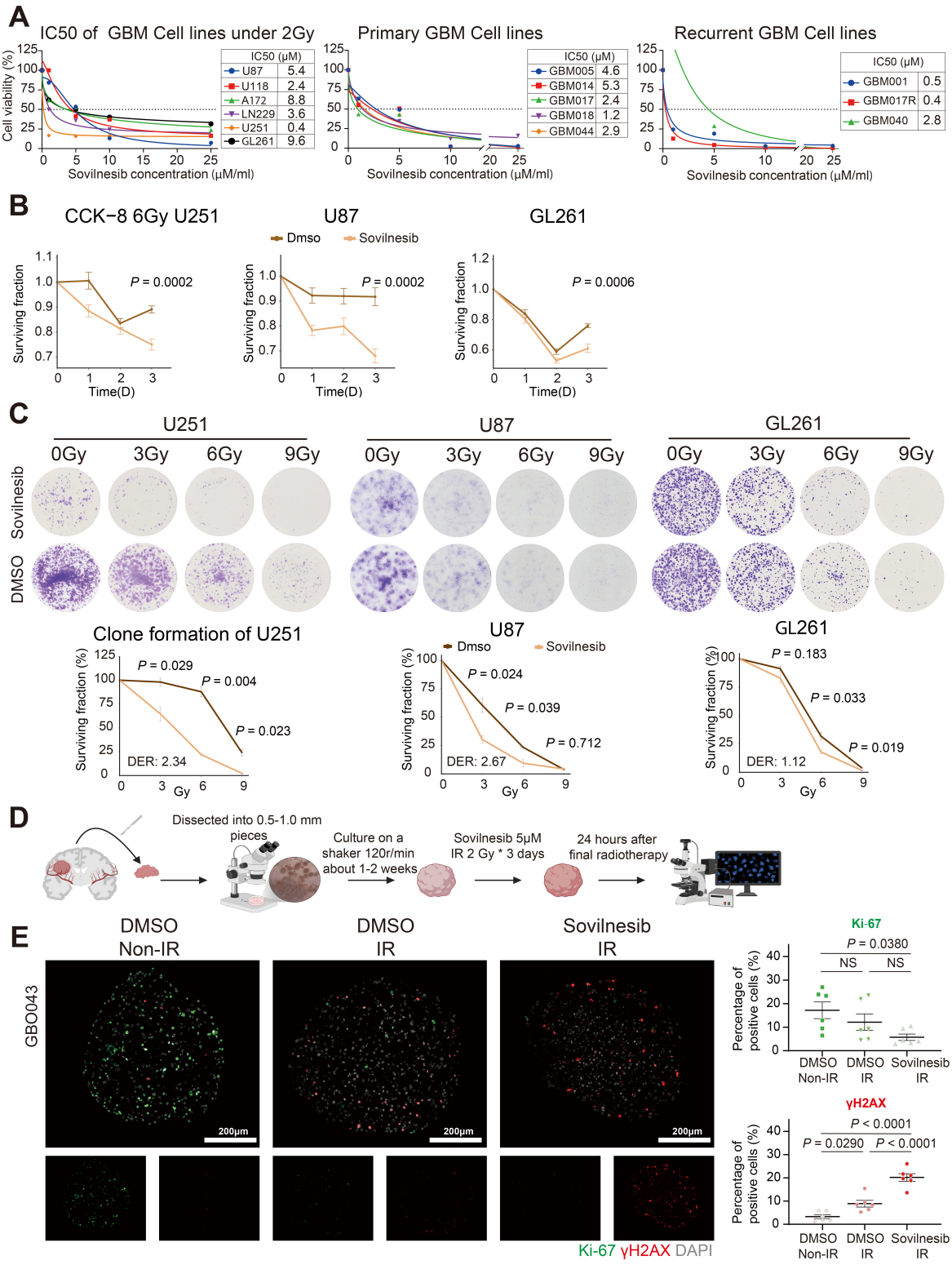


Figure 4

The KIF18A inhibitor sovilnesib sensitizes glioma cells and patient-derived organoids to radiotherapy

A. Cell viability analysis and IC_{50} of glioma cell lines treated with sovilnesib under 2 Gy irradiation.

B. Time-course survival curves of U251, U87, and GL261 cells treated with sovilnesib following 6 Gy irradiation (n = 6). Data represent mean ± SD.

C. Representative colony formation images and quantification of colony numbers in U251, U87, and GL261 cells treated with sovilnesib and irradiation (n = 3). Data represent mean ± SD.

D. Schematic illustration of GBM organoid generation and treatment with sovilnesib and radiotherapy.

E. Representative immunofluorescence images and quantification of Ki-67 (green) and γH2AX (red) expression in GBM organoids (n = 6). Data represent mean ± SEM. Statistical analyses: Student's t-test (B and C), one-way ANOVA test (E)

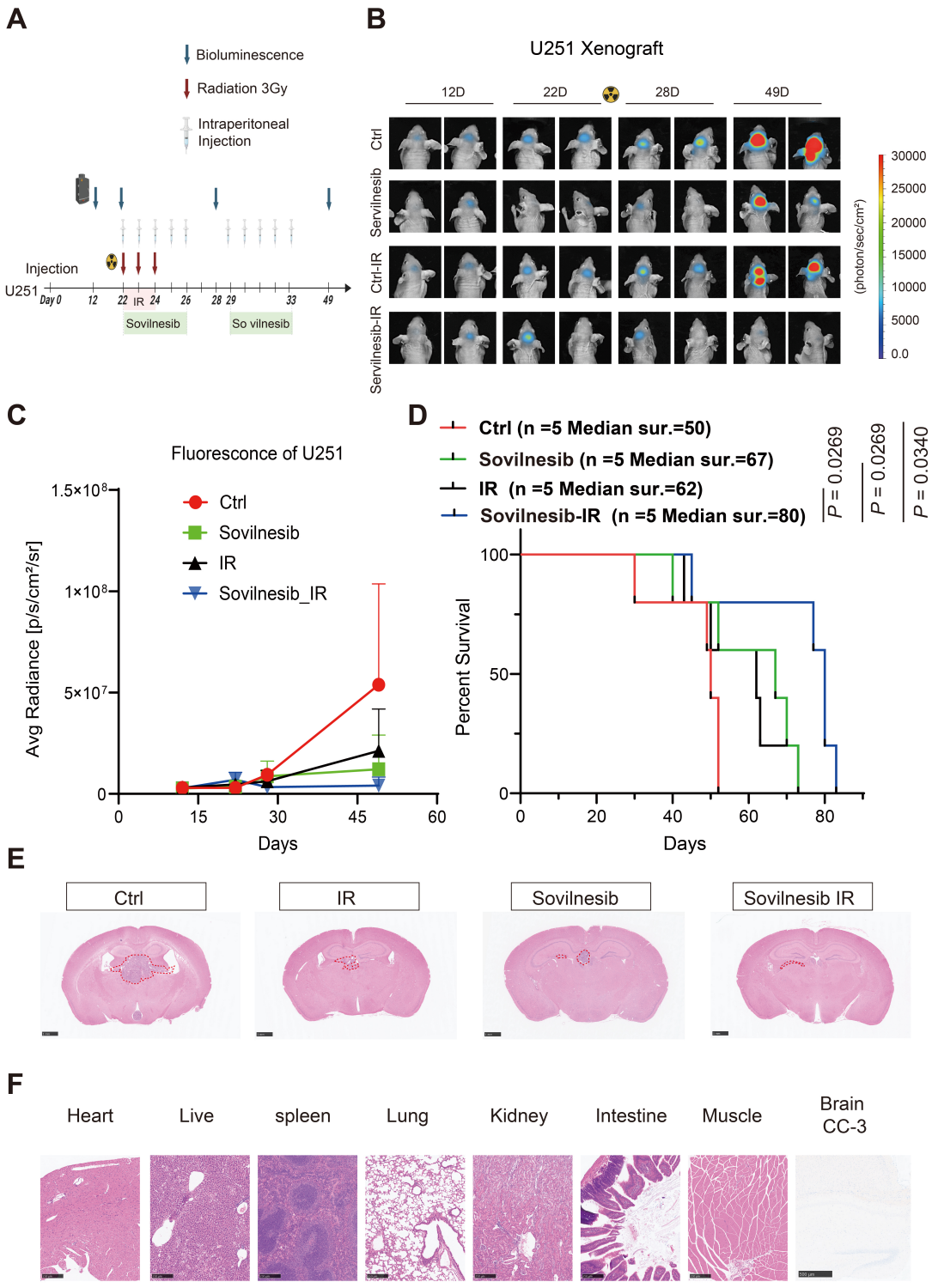


Figure 5

Sovilnesibprolongs the median survival of glioma xenograft models

A. Schematic illustration of treatment regimen for glioma xenograft models with radiotherapy and sovilnesib.

B. Representative bioluminescence images of mice bearing U251 intracranial xenografts.

C.Quantification of bioluminescent tumor signal in U251 xenografts following treatment. Data represent mean ± SD.

D.Kaplan–Meier survival curves of mice (n = 5).

E.Representative H&E staining of U251 xenografts on day 30.

F. Representative H&E staining of major mouse organs and immunohistochemical staining of brain tissues from treatment groups, showing no detectable tissue damage.

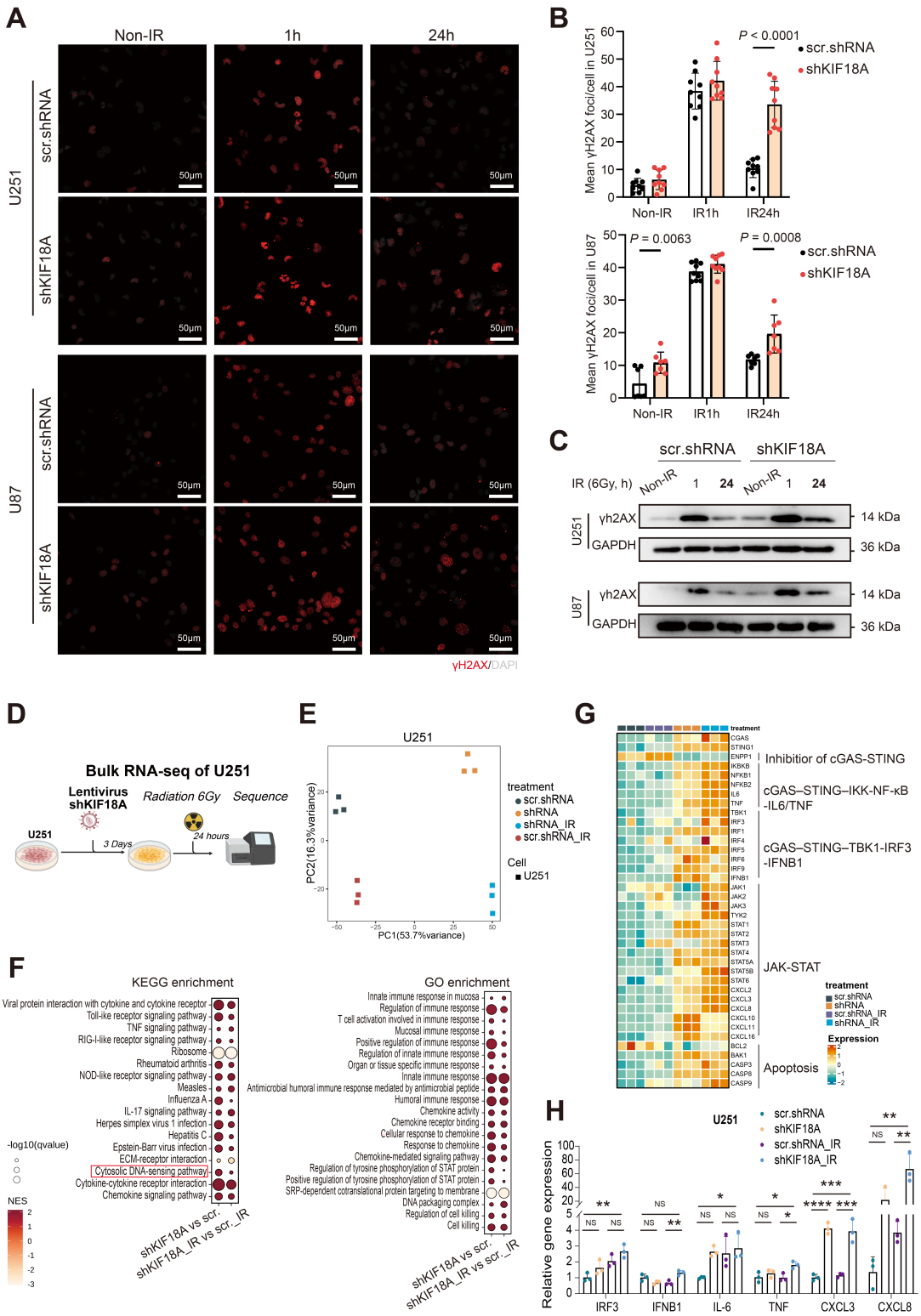


Figure 6

KIF18A inhibition increases DNA damage and enhances activation of the cGAS-STING pathway

A.Representative immunofluorescence images of γH2AX foci in U251 and U87 cells.

B. Quantification of γH2AX foci shown in panel A (n = 7–9). Cells containing ≥10 foci are plotted.

C. Representative Western blotting images of γH2AX expression in U251 and U87 cells following irradiation.

D. Schematic illustration of bulk RNA-seq in U251 cells.

E. PCA plot showing transcriptional differences among treatment groups.

F. Left: KEGG pathway enrichment analysis. Right: GO biological process enrichment analysis.

G. Heatmap of cGAS–STING pathway–related genes across U251 treatment groups.

H. RT–qPCR quantification of IRF3 and cytokine expression in U251 cells (n = 3). Statistical analysis: Student's t-test (B); one-way ANOVA (H). Data represent mean ± SD.

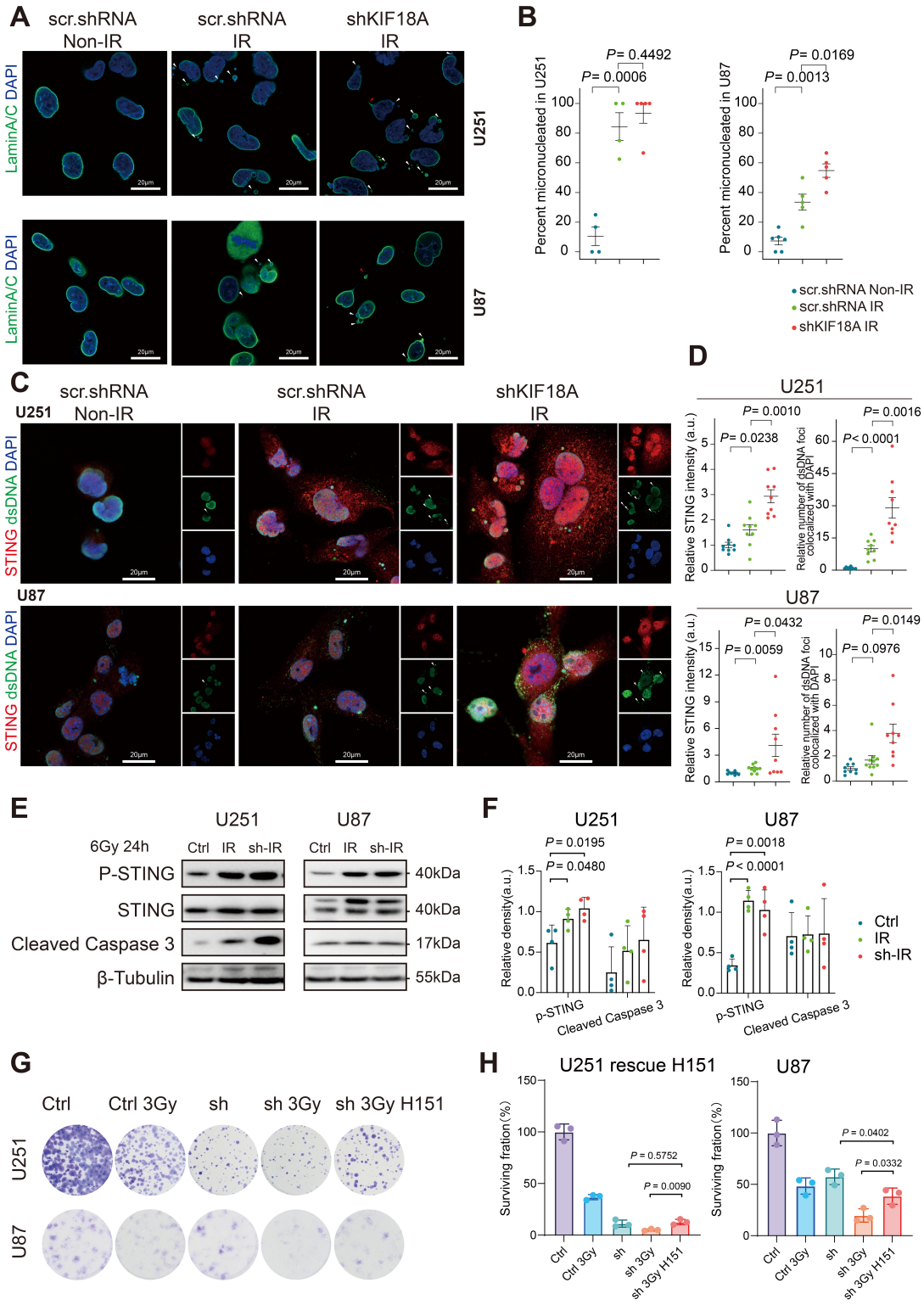


Figure 7

KIF18A inhibition induces micronucleus formation to accelerate cGAS-STING pathway activation

A.Representative immunofluorescence images of Lamin A/C in U251 and U87 cells. White arrows indicate micronuclei, and red arrows indicate lagging micronuclei.

B. Quantification of cells containing micronuclei (n = 4–6). Data represent mean ± SEM.

C.Representative immunofluorescence images of cytosolic dsDNA (green) and STING (red) in U251 and U87 cells.

D. Quantification of STING fluorescence intensity and cytosolic dsDNA foci (n = 9). Data represent mean ± SEM.

E.Representative Western blotting images of phosphorylated STING and cleaved caspase-3.

F. Quantification of Western blotting results shown in panel E (n = 4). Data represent mean ± SD.

G. Representative colony formation images of U251 and U87 cells.

H. Quantification of colony numbers shown in panel G (n = 3). Data represent mean ± SD.

Statistical analysis: one-way ANOVA (B, D); Student’s t-test (F, H).

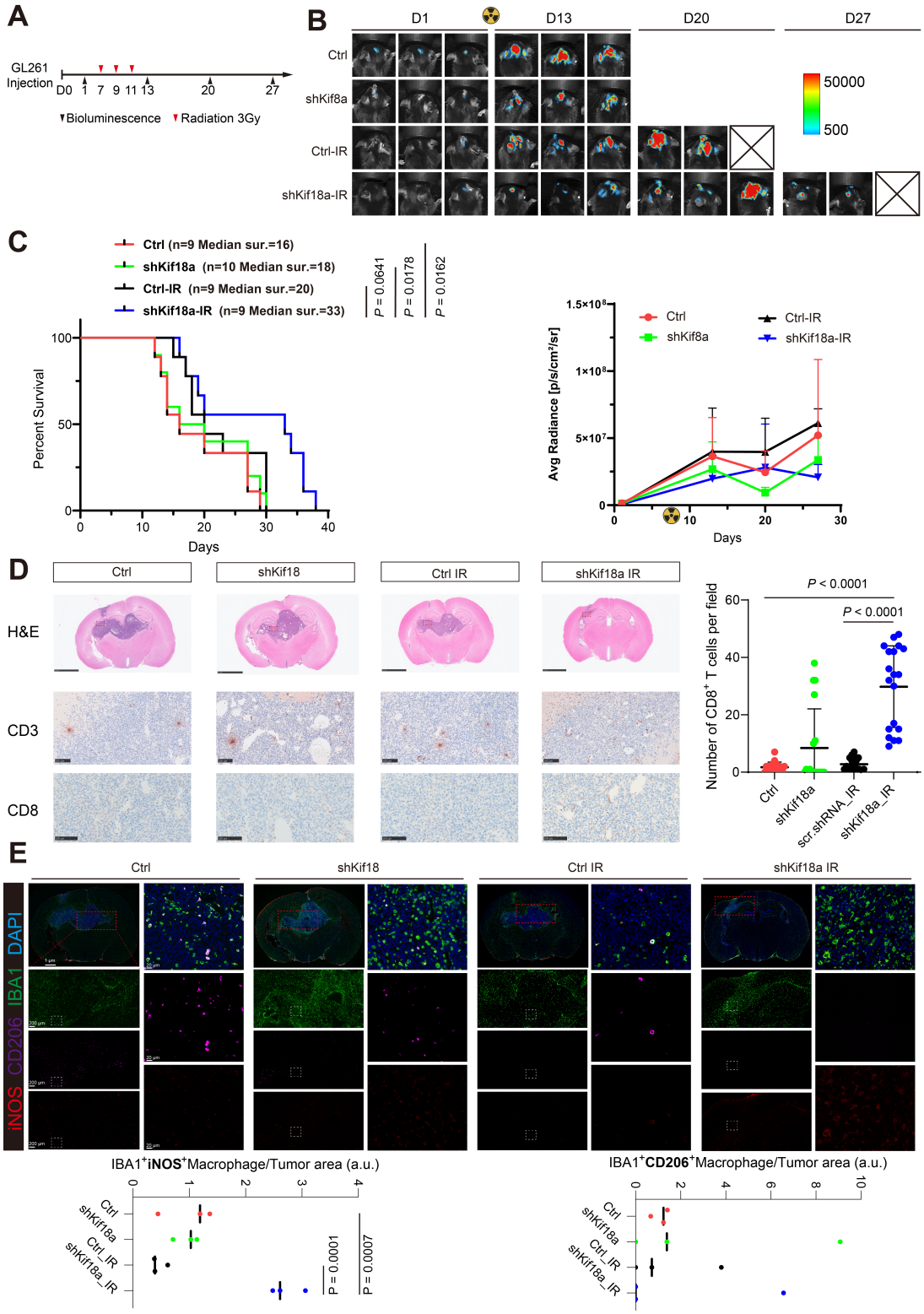


Figure 8

KIF18A inhibition enhances immune infiltration and macrophage M1 polarization

A. Schematic illustration of treatment regimen for GL261 glioma models.

B. Representative bioluminescence images of mice bearing GL261 intracranial xenografts.

C.Kaplan–Meier survival curves of mice (left) and quantification of bioluminescent tumor signal (right). Data represent mean ± SD.

D.Representative H&E staining and IHC staining of CD3 and CD8 in GL261 allografts (left). Quantification of CD8+ T cell per field (right). Data represent mean ± SD.

E.Representative staining image of IBA1, iNOS, and CD206 in mouse brains under different treatments (top) and quantification of protein level normalized to the control group (bottom). Each data point represents one mouse (*n* = 3 mice for each treatment). Data represent mean. Statistical analysis: one-way ANOVA (D, E).

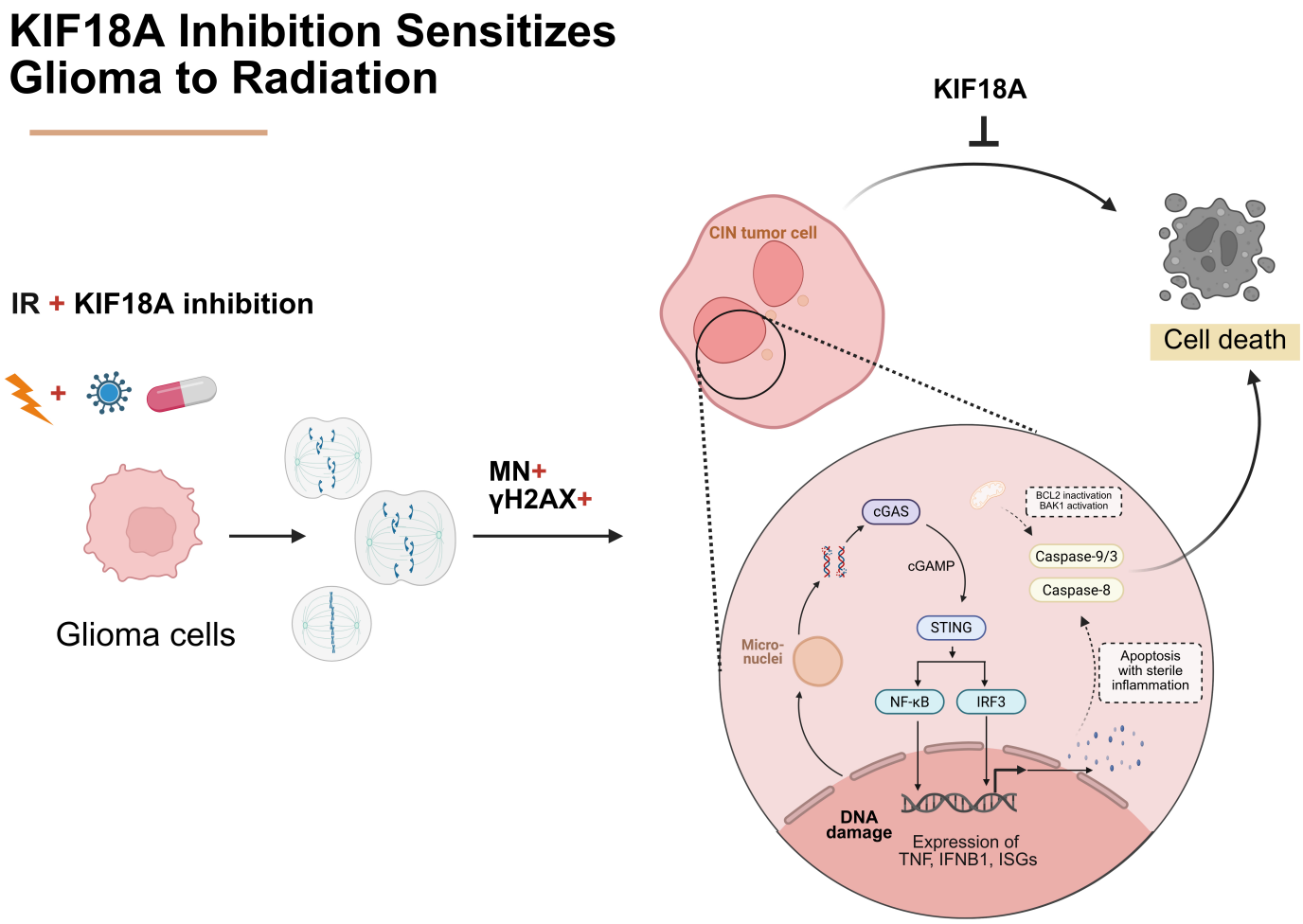


Figure 9

KIF18A inhibition sensitizes glioblastoma to radiation

Ionizing radiation induces mitotic chromosome mis-segregation and generates CIN tumor cells[20]. KIF18A inhibition similarly disrupts chromosome segregation and preferentially suppresses CIN-dependent tumor cells[17, 18, 60]. In combination, KIF18A inhibition increases micronucleus formation and cytosolic dsDNA release, leading to enhanced activation of the cGAS–STING pathway and induction

of apoptosis. Dashed arrows and boxes indicate mechanisms that require further investigation[55]. IR, Ionizing radiation; MN, Micronuclei; IFNB1, Interferon Beta 1; ISG, interferon-stimulated gene.

Supplementary Files

This is a list of supplementary files associated with this preprint. Click to download.

- SupplementaryFigure1.jpg
- SupplementaryFigure2.jpg
- SupplementaryFigure3.jpg
- SupplementaryFigure4.jpg
- SupplementaryFigure5.jpg
- SupplementaryFigure6.jpg
- SupplementaryTable1.xlsx
- SupplementaryTable2.csv
- SupplementaryTable3.xlsx
- graphicalabstractKIF18A.jpeg